80
CENTRAL RESEARCH LIBRARY
DOCUMENT COLLECTION

OAK RIDGE NATIONAL LABORATORY
operated by
UNION CARBIDE CORPORATION
NUCLEAR DIVISION
for the
U.S. ATOMIC ENERGY COMMISSION

LOCKHEED MARTIN ENERGY RESEARCH LIBRARIES
3 4456 0513744 7

ORNL-TM-2631

A TURBULENTLY HEATED ELECTRON PLASMA

W. L. Stirling and I. Alexeff

OAK RIDGE NATIONAL LABORATORY
CENTRAL RESEARCH LIBRARY
DOCUMENT COLLECTION
LIBRARY LOAN COPY
DO NOT TRANSFER TO ANOTHER PERSON
If you wish someone else to see this document, send in name with document and the library will arrange a loan.
UCN-7169
(3 3-67)

[This paper will be submitted for publication in Plasma Physics (Pergamon Press)]

NOTICE This document contains information of a preliminary nature and was prepared primarily for internal use at the Oak Ridge National Laboratory. It is subject to revision or correction and therefore does not represent a final report.

LEGAL NOTICE

This report was prepared as an account of Government sponsored work. Neither the United States, nor the Commission, nor any person acting on behalf of the Commission:

A. Makes any warranty or representation, expressed or implied, with respect to the accuracy, completeness, or usefulness of the information contained in this report, or that the use of any information, apparatus, method, or process disclosed in this report may not infringe privately owned rights; or

B. Assumes any liabilities with respect to the use of, or for damages resulting from the use of any information, apparatus, method, or process disclosed in this report.

As used in the above, "person acting on behalf of the Commission" includes any employee or contractor of the Commission, or employee of such contractor, to the extent that such employee or contractor of the Commission, or employee of such contractor prepares, disseminates, or provides access to, any information pursuant to his employment or contract with the Commission, or his employment with such contractor.

A TURBULENTLY HEATED ELECTRON PLASMA*

W. L. Stirling and I. Alexeff

Oak Ridge National Laboratory
Oak Ridge, Tennessee

ABSTRACT

The objective of this work was to produce a dense, ionizing plasma which could be used to shield a central hot ion plasma core against the influx of neutral gas or impurities. For a plasma to be an effective shield against Franck-Condon neutrals (spontaneously generated, energetic hydrogen atoms), the plasma density times the atomic neutral mean free path should be equal to or greater than 10^{14} particles/cm^2. We have developed a unique, high-energy, high density electron plasma annulus which exists in a magnetic mirror of 2:1 ratio and operates in hydrogen gas at pressure of 3×10^{-5} torr. The hot electrons are produced in a high voltage reflex discharge, or "arc." The arc electrodes are placed off the magnetic axis in the throats of their respective mirror coils. When heating takes place, the hot electrons are trapped in the magnetic mirror field and drift azimuthally due to the $\nabla B \times B$ precession. In this way a hot electron plasma annulus is created about the magnetic axis of the machine. Three different electron energy distributions have been observed simultaneously: One of 10^9 to 10^{10} cm^{-3} density at about 100 keV electron temperature; a second of 10^{11} to 10^{12} cm^{-3} density at about 2 keV electron temperature;

---

*Research sponsored by the U. S. Atomic Energy Commission under contract with the Union Carbide Corporation.

LOCKHEED MARTIN ENERGY RESEARCH LIBRARIES

3 4456 0513744 7

the third is the cold plasma of a few eV for the electron temperature at a density greater than 10^{12} cm^{-3}. An increase in magnetic field by a factor of 3 reduces the electron density in the annulus by a factor of about 5; however, the hot electron density generated at the main arc column is not appreciably affected. The plasma density in the annulus is about a factor of 50 too low to be an effective shield against Franck-Condon neutrals. Diffusion measurements show that the observed diffusion rate is much greater than classical and equals the Bohm rate for about 100 eV electrons.

I. INTRODUCTION

The objective of this work was to produce a dense, ionizing or environmental type of plasma which could be used to shield a central hot ion plasma core against the influx of neutral gas or impurities. A difficult component of the neutral gas present in the machine is the energetic atom resulting from dissociation of the deuterium or hydrogen molecular ion. These atomic neutrals known as Franck-Condon neutrals may have energies up to 3 to 7 eV. For a plasma to be an effective shield against them, the plasma density times the atomic neutral mean free path should be equal to or greater than 10^{14} particles/cm^2.

We have developed a unique, high-energy, high-density electron plasma annulus which exists in a magnetic mirror of 2:1 ratio and operates in hydrogen gas at pressure of 3×10^{-5} torr. As earlier reported (Stirling et al. (1966)) the source of the plasma is a reflex discharge. This type of discharge has been used to heat electrons before (Alexeff et al. (1964), (1966)) at ORNL. In the

present application, we placed the arc electrodes off the magnetic axis but still in the throat of their respective mirror coils. When heating takes place, the hot electrons are trapped in the magnetic mirror field and drift azimuthally due to the 7BxB precession. In this way a hot electron plasma annulus is created about the magnetic axis of the machine. The diameter of this annulus is about 18 inches at midplane of the mirror. By probing the plasma at different azimuthal positions, it is possible to study the heated plasma in regions far removed from the heating zones of the reflex arc. We discuss in this article the electron density and temperature produced in the annulus and the methods by which these measurements were made. The effect of magnetic field variation on the hot electron annulus is described. We also present the measured diffusion coefficient for the plasma in the annulus at a point 270° in azimuth from the reflex arc.

Figure 1 shows an axial cross-sectional view of the Beam Plasma Facility with two arc discharges separated by 180° in azimuth. Both the anode and cathode of either discharge is located just inside the center plane of one of the mirror coils. Bombarding ions maintain the necessary temperature for filament emission. The beam electrons are accelerated across the approximately 5/8" gap between cathode and anode, pass through the electrically-grounded, gas-fed anode and travel along the magnetic field to the electrically-isolated anticathode. The hollow, cylindrical anticathode is gas fed, approximately three inches deep, water cooled and is surrounded by a shaped iron sleeve in order to expand the beam and dissipate the collimated beam energy over a large area.

The production of the hot electron plasma depends primarily on magnetic field strength, gas feed rate and accelerating voltage once the cathode and anode are aligned in the magnetic field. With a relatively large anode bore, 5/8" inner diameter, the discharge operates best at a magnetic field of 2 to 2.4 kilogauss, axial midplane value, and an accelerating voltage of 7 to 10 kV. Under these conditions, the hot electron density is between 10^7 cm^{-3} and 10^8 cm^{-3} at a temperature of about 100 keV. With an anode inner diameter of 1/4", the discharge runs very reliably at an accelerating voltage of 28 kV. We have run as high as 40 kV. In the high voltage regime, the magnetic field must be somewhat lower--in the range of 1.6 to 2 kG. Three different electron energy distributions have been observed simultaneously under these operating conditions. Table I lists the electron density and temperature for each of the three. All of the observations discussed below pertain to operation under the 28 kV operating voltage condition.

II. GENERAL OPERATING CONDITIONS

Dependable operation of the discharge in the electron heating mode is obtained over a rather small range of the parameters of magnetic field, gas pressure, and accelerating voltage. Regardless of gas pressure or arc voltage, the discharge will not run stably above 1800 gauss due to arc-over sometimes resulting in damage to the anti-cathode. Maximum power input to the electrons is dependent on gas pressure and arc voltage and occurs at fields between 1500 and 1800 gauss, the actual value varying in an unclear

Table I. Temperature and Density Measurements and Methods

ENERGY	ELECTRON DENSITY	DENSITY METHOD	ELECTRON TEMPERATURE	TEMPERATURE METHOD	SECTION
Low	$>10^{12}$ cm^{-3}	Power balance to end probe, Langmuir probe, microwave cut off	Few eV	Langmuir probe	II, IV
Intermediate	$\sim 5 \times 10^{11}$ cm^{-3}	Power probe, saturation current, turnoff	~ 2 eV	Langmuir probe, power probe, turnoff	III
High	10^{9}-10^{10} cm^{-3}	X-ray flux	~ 100 keV	X-ray spectrum	III

manner. The power input to the electrons drops rapidly with decreasing magnetic field and is 20% to 25% of maximum at a midplane field of about 1000 gauss. Pressure is measured by an ionization gage mounted on the diffusion pump manifold. Operating pressure has been as low as 1.5×10^{-5} torr but is usually 3×10^{-5} torr. Below 1.5×10^{-5} torr operation is interrupted by arc over similar to that which occurs at high magnetic field. Power input to the electrons decreases rapidly with increasing pressure. A perforated cylindrical copper liner (not labeled in Figure 1) maintained at liquid nitrogen temperature during operation. This liner encloses the region between the mirror coils and separates both the reflex arc and heated electron plasma from the pump manifolds. When cold, the liner increases the power input to the electrons by a factor of five to ten with no significant pressure change at the ionization gage. No doubt the improved performance is due to the removal of impurities from the hydrogen gas present in the plasma region.

With our arc electrode geometry, there is no appreciable electron heating below 20 keV. At 22 to 24 keV, the hot electron annulus becomes clearly visible and at 26 to 28 keV, between 5 and 10% of the arc input power is transferred to the hot electrons. Arc current under these conditions is 800 mA to 1000 mA. Without excessive radial losses, the power in the hot electron annulus should end up on the end plates due to plasma scattering out the mirrors.

We have made power accountability measurements when operating at 17 kW to 24 kW input power levels. With either arc operating with equal gas feed into the anode and anti-cathode, we can account for about 85% of the input power: 50% to 65% on the anti-cathode; 5% to 7% on the end plates on which the plasma streaming out the ends terminates; and 15% to 25% on the anode. Only a few hundred watts is required to keep the cathode filament emitting. With all the gas feed into the anode, the power dissipated on the anti-cathode is lowered to about 10% of the input power, and the end plates receive the power that was going to the anti-cathode. Since there is no increase in the electron saturation current streaming from the annulus, out the mirrors, and since the x-ray intensity increases only about 25%, we believe that the increased power to the end plates is due primarily to a partial blow up of the reflex discharge and not due to a significant increase in hot electron density in the annulus. At high power dissipation on the anti-cathode, the anti-cathode floats at approximately ground potential, which is anode potential. Thus, the primary electron stream must scatter across field lines to the anode or grounded end plates. One would expect the observed increase of power on the end plates under these conditions.

III. PLASMA DENSITY AND TEMPERATURE

The hot electron energy distribution has been observed with an x-ray scintillation spectrometer. The three inch NaI(Tl) crystal and photomultiplier were well shielded from any stray

magnetic fields and were contained in 6-in. thick lead cylinder. The volume of plasma examined by the spectrometer was chosen by means of a lead collimator which at no time allowed x-rays from the arc electrodes or main arc column to reach the crystal. The line of sight of the collimator was perpendicular to and through the center of the annulus. The line of sight terminated in a large pump manifold such that wall x-rays were virtually non-existent.

We have concerned ourselves primarily with measurements of the intermediate and low-energy electron distributions listed in Table I. We observe from plasma x-ray total intensity measurements that the density of the 100-keV energy electron component is in the range of 10^9 to 10^{10} cm^{-3}.

A great deal of difficulty is encountered when measuring the properties of the intermediate-energy electrons. The intermediate-energy component is defined as those electrons of energy sufficient to ionize the background gas but insufficient to produce x-rays of sufficient energy to be detected by our scintillation spectrometer, i.e., less than 15 keV to 20 keV. The presence of these electrons may be easily observed by inserting a paddle or probe into the annulus. The x-ray producing distribution is wiped out, but the background gas is still being ionized, as evidenced by the existence of the glowing annulus and by the streaming of cold plasma out the mirrors. We have measured the power delivered to the probe by the electrons drifting in the annulus.

The power probe consists of a water cooled 1/4 inch diameter copper rod, which is free to protrude through but not touch a water cooled copper jacket. The entire assembly is movable through the annulus during operation. By adjusting the length of rod exposed, usually 1/4" to 3/8", we can make differential power measurements of the annulus.

Figure 2 shows three curves related to the position of the power probe relative to the annulus. Curve 1 shows the power, measured calorimetrically, delivered to the probe in a radial cross section at midplane. Curve 2 shows the ion saturation current streaming out the mirror. Figure 3 shows the relative positions of the probes. The current probe traversed the entire radial extent of the annulus. The ion saturation current behavior shows that the presence of the power probe lowers the electron density of the annulus by about 30%. Curve 3 of Fig. 2 shows the decrease of x-ray intensity (x-rays originating in the plasma annulus) as the power probe is inserted into the annulus.

The power delivered to the probe allows us to calculate the average electron density of the plasma contained in the flux tube which is intercepted by the probe. One must be careful to use the cross sectional area of the intercepted flux tube in the calculation since the probe wipes out the plasma in this flux tube. Thus

$$\text{Power} = n_e E_\perp (\ell \cdot L) V_d \qquad (1)$$

where n_e is the electron density, $E_\perp$ is the energy per electron due to its motion perpendicular to the magnetic field, $\ell \cdot L$ is the flux tube cross sectional area (probe length times flux tube length) and V_d is the electron drift speed. However, the drift speed in

the existing magnetic field gradient is proportional to the energy of the particles. Assuming an average velocity for the electrons, the density is inversely proportional to the square of the energy for a given power dissipation. Thus an independent measurement of the electron drift speed, or energy, is needed to determine the electron density from the power per unit area delivered to the probe:

$$\text{Power} = \frac{n_e E^2}{e} \times \frac{\nabla B}{B^2} \qquad (2)$$

We can impose an upper and lower limit to the temperature or energy of the intermediate-energy electrons. An energy upper limit is determined by the fact that the electrons are non x-ray producing: $E_{max} \leq 20$ keV. A lower limit can be determined from the assumption that the electron drift time for one revolution of the annulus is of the order of, or shorter than, the scattering time of the electrons out the mirrors which is about 200 μsec. This assumption is reasonable, since there is negligible decay of the plasma with azimuth. This condition requires that $E_{min} \gtrsim 2$ keV.

Langmuir probe studies of the plasma annulus on the midplane indicate two electron distributions. Figure 4 shows a linear plot of the voltage current characteristic. The long sloping tail at high negative voltages has been investigated out to 3 kV, but ion saturation is still not achieved. The conventional semi-logarithmic plot yields an electron distribution with a mean energy of 100 eV. Extrapolation of the curve beyond -3 kV yields a value of the ion saturation current which, when subtracted from the meter

reading, gives an electron current vs voltage characteristic. This characteristic shows the existence of another electron distribution with an electron temperature of 1.75 keV.

An attempt was made to measure the electron drift speed by perturbing the reflex discharge and looking at the resulting effect on a current probe 180° in azimuth away. A density perturbation should precess around the annulus, yield a direct measurement of the precession velocity due to the magnetic field gradient, and hence the electron energy. The oscilloscope traces are difficult to interpret, possibly due to voltage pickup other than that from the desired current variations. These measurements yield an electron energy that appears to be about 4 to 5 keV.

The basic principle of the measurement is best understood with the aid of the sketch in Fig. 5 for single arc operation. An interesting feature of the plasma annulus or blanket formed by the hot-precessing electrons is that it cannot be completely uniform in azimuth. Plasma generated in the arc is lost during the precession around the machine, both by being scattered out the mirrors and by being absorbed on probes. Thus, the azimuthal density profile has a "step" at the position of the arc, as is shown in Fig. 5. Now, if the arc is turned off in a time less than or comparable to the precession time of the plasma around the machine, the plasma will be left in its stepped form. We then expect the step to rotate around the machine with the velocity of the precession. This step in plasma density should be detected by probes present in the plasma ring.

An example of the precessing disturbance is shown in Fig. 6. The top and bottom beams represent probes at 90° and 270° in azimuth, respectively. The weak ripple in each decay curve is the desired signal. This ripple cannot be a.c. pickup for three reasons: (1) the amplitude of the ripple dies away as the plasma is lost; (2) the frequency of the ripple decreases with time; (3) the phase of the two signals differs by 180°, as is expected for a precession disturbance. (Note that the two signals are slightly displaced in time for t = 0 due to an oscilloscope misadjustment.) Though the desired signal is weak, it has been observed many times and can therefore be used as a method of determining the frequency of rotation.

Knowing the frequency of the precessing disturbance, we can easily find the perpendicular electron energy from the equation shown below:

$$V_g = 2\pi \quad rf = \frac{E_{\perp}}{eB}\left[\frac{\Delta B}{B}\right] \tag{3}$$

Here, V_g is the precessional velocity, r is the radius of the plasma ring where precession is occurring, f is the frequency of precession, E is the energy of the average electron, stored in motion normal to the magnetic flux lines, $\frac{\nabla B}{B}$ is the magnetic field gradient at the position of the precessing electrons, e is the electron charge, and B is the magnetic field. Data used in the calculation are as follows: r = 22 cm, $f = \frac{1}{70 \times 10^{-6}}$ sec (2nd and 3rd bounce on top trace), B = 1550 G, $\frac{\nabla B}{B} = .0067\ cm^{-1}$. $V_g \approx 2 \times 10^{6}$ cm/sec. Solving for $E_{\perp}$ we find that $E_{\perp}$ = 4.6 keV.

Other features of interest are first, the persistence of the step during several cycles, which suggests that the electrons may have a rather narrow energy distribution and second, the decrease of frequency with time, suggesting that the electrons are cooling as time progresses.

Our measured values of the intermediate energy electron distribution range from a maximum of 4.6 keV to a minimum of 100 eV. For the sake of calculation of the electron density by equation (2), we have chosen an energy of 2 keV which yields a value of 5×10^{11} cm^{-3}.

An independent determination of the electron density can be made. Knowing the gas density inside the machine and measuring the rate of flow of secondary plasma out the mirrors of the machine, one can compute the generation rate of secondary plasma inside the machine.

$$\frac{dn_+}{dt} = n_o n_e < \sigma v > - \frac{j \cdot A}{eV} \qquad (4)$$

At equilibrium

$$n_o n_e < \sigma v > = \frac{j \cdot A}{eV} \qquad (5)$$

where j is the ion saturation current density, A is the area of the plasma, V is the plasma volume, n_+ is the ion density, n_e the electron density, and n_o the neutral density. Since $< \sigma v >$ for ionization is approximately independent of energy for electrons having energies greater than 100 eV, the density of ionizing electrons is easily calculated to be about 2×10^{11} cm^{-3}. This figure

is in good agreement with the density figure of 5×10^{11} cm^{-3} determined above from the power probe.

We employed a 3 cm microwave cutoff experiment in order to measure the electron density in the annulus. The transmitting horn was placed inside the precessing ring of hot plasma and was oriented to look through the shell, at midplane, to the receiving horn about 6 inches away. It was possible to show a severe attenuation of the transmitted microwave power. Thus, the density of the total electron population is greater than 10^{12} cm^{-3}.

We made an attempt to determine if the ions in the annulus were being heated. We looked spectroscopically for evidence of a Doppler shift in the recombination radiation. There was no significant heating, and we placed an upper limit of 10 eV for the ion energy.

IV. EFFECT OF SATURATION CURRENT MEASUREMENTS OF PLASMA DENSITY

An interesting observation has been made when measuring the electron saturation current which may be useful for increasing the energy and possibly the density of the intermediate-energy electron group. The method utilizes the same tantalum wire probes used for monitoring the electron saturation current streaming out the mirror. With the high plasma density recently achieved in the shell, an application of a positive voltage on the current probe to measure the electron saturation current causes a spreading of the shell and a change in power delivered to the power probe.

Figure 3 indicates the positions of the current probe and midplane power probe. Both are located about 90° (azimuth) from the streaming electron beam of the reflex discharge.

The total power delivered by the arc power supply is 25 kW and the total power input to the undisturbed shell is about 2 kW or roughly 8% of the arc power input. The bias voltage increased the power input to the shell by about 20% and the r.f. signal made an increase of about 30%, an average of about 600 W. In either case, the power input to the tantalum wire probe is about 100 W or about 1/6 of the power increase to the shell. Thus the source of the increased energy to the shell must be the primary arc supply with the conversion efficiency increasing from about 8% to 10%.

There is a variation in the power delivered to the probe with frequency. The d.c. bias causes a decrease in the peak power and more radial spreading of the plasma than the r.f. signal. The applied r.f. frequency is not critical but seems to have a maximum heating effect below 300 kc and falls off slowly with increasing frequency. Since the period of a 300-kc signal is about equal to the transit time of the cold plasma electrons (1 to 2 eV) out of the machine, it is possible that the plasma heating and spreading is being driven by an oscillation of the cold plasma. Another possible explanation may be related to the fact that the frequency of rotation due to the $\nabla B \times B$ drift of the hot electron distribution around the axis of symmetry of the device is also about 300 kc. Figure 7 shows that the effect of the applied r.f. is not

observable after the power probe intercepts about 1/2 of the annulus. Figure 2 shows that this is also the position of the probe at which the hot electron distribution is wiped out as evidenced by the fact that the x-ray intensity is negligible.

Application of a negative voltage on the tantalum wire probe in the mirror throat to measure the ion saturation current has no noticeable effect on the power delivered to the power probe in the annulus. With no voltage applied, the tantalum heats to a temperature of 1800 to 2000° C, measured with an optical pyrometer. When a negative voltage is applied, the ion bombardment causes the wire to heat rapidly to electron emission temperature. Thus at the high plasma densities, we cannot run meaningful probe characteristics. However, we can make a rough calculation of the density of the plasma streaming out the mirror by equating the energy input to the tantalum wire to the energy radiated from the tantalum wire. The radiated energy, R, in watts cm^{-2} is given by the expression:

$$R = \epsilon\sigma T^4$$

where $\epsilon = 0.3$ for tantalum, $\sigma = 5.67 \times 10^5$ e.g.s. units, and T is the temperature in degrees K.

$$R = 40 \text{ watts/cm}^2$$

This power is supplied by the bombarding particles and is equivalent to

$$neV\ v_s$$

where n is the particle density, eV is the average energy per particle, and v_s is the streaming velocity out the mirrors.

If one considers the decay of the ion saturation current after arc turnoff to be equal to the time required for an ion to drift out of the mirror, the streaming velocity is directly measurable. An ion temperature of 1.4 eV is required for the transit time to be equal to the measured decay time of 0.3 msec. Expressing v_s in terms of energy, the density may be written

$$n = R \left[\frac{m_i}{2(eV)^3} \right]^{1/2}$$

$$n = 10^{13} \text{ cm}^{-3} \text{ for hydrogen.}$$

This value is in good agreement with the microwave cutoff experiment.

We can make an estimate of the effectiveness of the plasma annulus as a shield against Franck-Condon neutrals. From Fig. 7 we see that the thickness of the plasma annulus is about 2 cm. For a mean free path for the neutrals equal to 2 cm, the plasma electron density n_e, should be

$$n_e = \frac{10^{14}}{2} = 5 \times 10^{13} \text{ cm}^{-3}$$

Thus the density in the annulus is about a factor of 50 too low to be an effective shield against the energetic Franck-Condon neutrals. Our two-arc operation, section VII, was an attempt to make the annulus thicker and more dense. As discussed there, it was easy to double the annulus thickness but the density was not appreciably affected. The main arc column itself is about a factor of five thicker than the annulus. A hot electron density of 10^{13} in this region would make an effective shield against

energetic neutrals. Of course this would require the arc column to be oriented on the magnetic axis in order to be useful.

V. DIFFUSION OF THE PLASMA

An attempt has been made to measure the radial diffusion of the plasma escaping from the annulus. A current probe located on the midplane was moved radially through the annulus. The azimuth of the probe was 90° from either arc and was therefore best situated to study the diffusion from the blanket and not from the discharge column itself. However, we cannot rule out the influence of the main arc column on the diffusion measurements. We may interpret these measurements either as an upper limit on the diffusion coefficient from the hot electron plasma annulus or an estimate of the diffusion effects of the turbulent fields existing in the main arc column. Unfortunately, the perturbation of the plasma by the probe increases as the probe penetration into the blanket increases. Since the drift velocity of the plasma along the magnetic field is very much higher than the azimuthal drift in the magnetic field gradient, the probe completely wipes out all plasma at a radius greater than the radius of the probe tip and all plasma at an azimuth greater than 90° (measured from the arc in the direction of ∇B drift) for the entire length of the machine.

Figure 8 shows a semilogarithmic plot of the probe current vs radial position from annulus center. The probe was biased to measure the ion saturation current. The radial diffusion coefficient was calculated from that region of the curve for large

radius in order to minimize the perturbing effects of the probe in the plasma.

Under the model of Simon (1959), we may infer a value of the perpendicular diffusion coefficient from the e-folding length X_o. For planar geometry, Simon showed that the density varied as exp $(-X/X_o)$; for cylindrical geometry, this becomes $r^{-1/2}$ exp $(-r/r_o)$. In the present case, the ratio of the blanket thickness ΔR to the radius of curvature R is $\Delta R/R \approx 1/5 \ll 1$; so that we shall use the planar geometry. The e-folding length X_o and the diffusion coefficient $D_\perp$ are related by the following expression:

$$D_\perp = \frac{2vX_o^2}{L}$$

where v is the ion thermal speed and L is the length of the plasma. We wish to compare the observed diffusion coefficient to the "classical" value based on binary collisions with neutral gas atoms,

$$D_\perp(\text{classical}) = \frac{\lambda v}{3} \frac{1}{1 + \omega_c^2 \tau_{coll}^2}$$

where λ is the mean free path for scattering from neutrals, τ_{coll} is the mean free time between collisions, and ω_c the ion gyro-frequency. For cases of interest to us, $\omega_c^2 \tau_{coll}^2 \gg 1$, and we can write

$$D_\perp(\text{classical}) \approx \frac{2}{3} \frac{T_i}{eB} \frac{1}{\omega_c \tau_{coll}}$$

where T_i is the ion temperature and B is the magnetic field strength. Since the ion temperature is not well known

experimentally, we observe that $T_i \sigma \sim 30 \times 10^{-15}$ cm^2 eV for 10 eV $\lesssim T_i \lesssim$ 100 eV.

Our experimental values are $X_o \approx 2$ cm, $L \approx 150$ cm, $N_o \approx 2 \times 10^{12}$ cm^{-3}, and $B \approx 1.5$ kG; hence

$$\frac{D_\perp \text{ (observed)}}{D_\perp \text{ (classical)}} \approx 300.$$

Since the observed rate is so much larger than the classical rate, one might compare it to the Bohm rate.

$$D_{Bohm} = \frac{10^5 \, T_e}{16 \, B}$$

with T_e in eV and B in kG. For $V_i \approx 10^7$ cm/sec,

$$\frac{D_\perp \text{ (observed)}}{D_{Bohm}} \approx \frac{10^2}{T_e} \text{ eV}.$$

Since the proper value to use for T_e is in doubt in this case, we shall only point out that the observed diffusion rate equals the Bohm rate for 100 eV electrons. In any event, the diffusion is much faster than the classical rate, even if the diffusion is occurring in the main arc and not in the shell as assumed above. If one assumes the diffusion occurs primarily when the plasma passes through the main arc column (due to the turbulent heating fields) the classical value would be increased by 10^2 due to N_o but decreased by 30 due to L. Thus

$$\frac{D \text{ (observed)}}{D \text{ (classical)}} \approx 100$$

VI. INVESTIGATION OF MAGNETIC FIELD EFFECTS

We have made an attempt to generate the hot electron plasma in magnetic fields higher than the 1500 G to 1800 G axial midplane

value now attainable. In general, the interaction will not generate the blanket at magnetic fields above 1800 G. Raising the field higher has been observed to have the equivalent effect of reducing the resistance across the arc electrodes, causing the discharge to extinguish.

A 3/8 in. thick, 4-in. I.D. iron cylinder was placed around the anode to reduce the field in the anode channel. Thus a stronger magnetic field in the machine would be necessary to bring the field value in the anode channel back up to the original operating value. With this modification, it was found that the optimum axial midplane field value rose to about 1900 to 2000 G. The magnetic field reduction in the center of the anode is about 25%. In addition, the power input has been increased to about 40 kW.

Figure 9 shows the magnetic field present in the anode channel with a shaped 3/4-in. I. D. iron cylinder. The unperturbed field is also shown for comparison. The arrowheads indicate the spacing of the electrode surfaces, the anode being 5.5 in. long and the iron being 4.5 in. long. The cathode is positioned in the center of the 2:1 ratio mirror coil. With this arrangement we have successfully generated the blanket at a midplane magnetic field of 4000 G, although operation is much more steady at 3000 to 3300 G. Under the operating conditions of Fig. 9, the axial midplane field is about 3000 G. This is about the same value of field in the anode when operating at 1500 G axial midplane field with no iron shielding about the anode. These results may indicate

the presence of an instability in the anode region of the type studied (Hoh (1963)) or (Simon (1963)) which extinguishes or shorts out the discharge at sufficiently high magnetic fields. Estimates of the intermediate-energy electron density are a factor of 2 to 3 down from that obtained with 1500 G with no iron shielding. As shown at the end of this section, however, the hot electron density remains constant in the region of the main arc column. The interaction with iron shielding is not nearly as critical to parameter adjustments with magnetic field as is the case with no shielding.

Attempts to achieve a power input in the vicinity of 40 kW resulted in destruction of the anode. The inner wall of the anode melted at the location of the maximum magnetic field, point A.

Figure 10 shows an anode and a field-producing coil which was used to replace the original anode and iron shield. This coil is capable of bucking out an applied magnetic field of about 18 kG, which is the maximum attainable with the present mirror configuration.

Figure 11 shows a typical field shape obtained with the bucking coil when the axial midplane field is 2000 G. The bucking coil has two advantages over the iron shield previously used to reduce the field in the anode region. First, we can continuously vary the magnetic field strength in the anode channel while operating. Second, the coil does not produce regions of enhanced field, which the iron does produce just outside either end of the iron cylinder. The coil effectively reduces the mirror ratio along the flux lines of the discharge column.

We achieved a significant increase in magnetic field with the bucking coil energized. However, the density of the hot plasma in the annulus at the point of measurement decreased by about the same factor. The density at the main arc column remained constant. The results observed with the bucking coil may be summarized with the aid of Fig. 12. This figure shows the variation of three different physical parameters with the midplane magnetic field. The midplane field has been increased to 5500 G with the bucking coil on. The maximum obtained with the iron was 4000 G. However, the electron saturation current to a probe in a mirror coil throat fell by a factor of about 3 when using the bucking coil. At the same time, the operating pressure or neutral density increased by a factor of less than 2. Since the intermediate-energy electron density varies directly as the electron saturation current and inversely as the neutral density, the electron density decreased by a factor of about 5 for a magnetic field increase of 3.5. This density decrease arises from the fact that the grad B drift of the electrons varies inversely with magnetic field, and the relaxation time for scattering out the mirror varies inversely with neutral density. Thus, the hot electrons precess more slowly through a higher density of scattering centers. One can estimate the change in density of hot electrons being produced back in the main arc column at the higher magnetic field from the expression:

$$n = Ne^{-t/\tau}$$

where N is the trapped, hot electron density leaving the main arc column, n is the trapped, hot electron density at the probe, t is

the drift time from column to probe, and τ is the hot electron relaxation time for 90° scattering.

For the two magnetic field values, a = 1500 gauss and b = 5500 gauss, we have

$$\frac{N_a}{N_b} = \frac{n_a}{n_b} \; e^{(t/\tau)_b - (t/\tau)_a}$$

$$N_a = N_b \times \frac{n_a}{n_b} \; e^{(t/\tau)_a \left[\frac{t_b}{t_a} \; \frac{\tau_a}{\tau_b} - 1\right]}$$

Now $t = \frac{x}{V_d}$, where x = distance from arc to probe and V_d = drift velocity, $V_d \propto \frac{1}{B}$, where B = magnetic field. Also $\tau \propto \frac{1}{N_o}$, where N_o = neutral density. We have: x = 100 cm, $(V_d)_a = 10^6$ cm/sec (calculated), $\tau_a = 4 \times 10^{-4}$ sec (calculated for $N_o = 10^{12}$ cm^{-3}), $n_b = 5\ n_a$, $t_b = 3.5\ t_a$ and $\tau_a = 2\ \tau_b$. Substitution of these values into the above expression yields the result that:

$$N_a \approx N_b$$

That is, the trapped hot electron density at the arc is unchanged with increasing magnetic field.

Figure 12 also shows that the discharge operated at magnetic fields in the anode channel above the 4400 G maximum which can be achieved without the bucking coil on. With the bucking coil, the change in field shape in the anode channel apparently allowed us to operate at much larger midplane fields, with slightly higher fields in the anode channel. These results are somewhat different from those with the iron, which suggested that we could increase the midplane field only when the field in the anode channel was held at its initial value. These preliminary results with the

bucking coil suggest that the anode channel magnetic field is an important parameter in the resonance condition responsible for the electron heating observed. Both the coil and the iron shield result in an increase of the maximum magnetic field at which the heating process will operate.

VII. TWO ARC PERFORMANCE

The object of running with two arcs was to increase the radial thickness and density of the annulus. The schematic in Fig. 1 shows two arcs installed 180° in azimuth away from each other. We have run with the electrodes of both arcs displaced 6 in. from the magnetic axis. In this case, the primary effect is on the hot electron distribution. The x-ray intensity is increased by a factor of 10 or more over that for a single arc, while the power delivered to the power probe is less than the sum of that available from either arc alone. Figure 13 is a measure of the power delivered to the power probe for a 2-inch separation of the arcs: one is 6 in. off axis and the other 4 in. off axis. The two annuli are clearly separated. Compared with a single arc, there is an increase in x-ray intensity by a factor of 3 to 5 with both arcs operating.

The operating pressure is the same in either single or double arc operation. Thus optimum gas feed for single arc operation must be cut in about half when two arcs are run. One cannot compare two arc operation to one arc by simple turning off one of the arcs. In the comparisons made above, gas feed was adjusted

to give maximum hot plasma density for each mode of operation. Thus one would not expect the power probe readings to double from single to two arc performance. The effect of two arcs on the x-ray production, and consequently the high energy electron distribution is striking. We have not investigated this effect in detail.

VIII. CONCLUSIONS

We have successfully produced a hot electron plasma annulus in a magnetic mirror with at least two hot electron distributions: one of 10^9 to 10^{10} cm^{-3} density at about 100 keV electron temperature; a second of 10^{11} to 10^{12} cm^{-3} density at about 2 keV mean energy. The product of the annulus thickness and plasma density is about a factor of 50 too low in order for the annulus to be an effective shield against Franck-Condon neutrals. Five to ten percent of the input power is transferred to the trapped, hot electrons. We have found that the magnetic field in the anode channel is most important when an attempt is made to increase the axial midplane magnetic field above 2 kilogauss. By maintaining a reduced field in the anode channel, we have generated the hot electron annulus at midplane magnetic fields up to 5.5 kilogauss. The density of hot electrons in the annulus decreases by a factor of about five. However, the hot electron density generated at the main arc column is not appreciably affected. In this work some new and novel diagnostic techniques have been developed.

ACKNOWLEDGMENTS

We would like to thank W. D. Jones for his assistance in making the microwave measurements, Gareth Guest for helpful discussions concerning plasma diffusion and J. R. McNally, Jr., for his assistance in making spectroscopic observations. We would also like to thank R. V. Neidigh for many stimulating discussions.

REFERENCES

Alexeff, I., Neidigh, R. V., and Peed, W. F. (1964) Phys. Rev. 136A 68.

Alexeff, I., et al., Plasma Physics and Controlled Fusion IAEA, Vol. II (1966) 781.

Hoh, F. C., Phys. Fluids (1963) 6 1184.

Simon, A., Proc. U. N. Internt'l Conf. Peaceful Uses of Atomic Energy, 2nd, Geneva (1959) 32 343.

Simon, A., Phys. Fluids (1963) 6 382.

Stirling, W. L., et al., Plasma Physics (1966) 8 157.

FIGURE CAPTIONS

Fig. 1 Beam Plasma Facility.

Fig. 2 Measurements on Plasma Annulus with Power Probe.

Fig. 3 Isometric--Single Arc Operation.

Fig. 4 Voltage-Current Characteristic for Probe on Midplane.

Fig. 5 Azimuthal Plasma Density Profile.

Fig. 6 Probe Traces Showing Precessing Step.

Fig. 7 Plasma Spreading Due to a Positive Bias and to a 300-kc r.f. Drive on a Probe in Mirror.

Fig. 8 Variation of Ion Current with Radial Distance from Magnetic Axis for Probe at Midplane.

Fig. 9 Variation of Longitudinal Magnetic Field Intensity in Anode Channel. Axial midplane field about 3100 G.

Fig. 10 Schematic of Anode-Cathode Assembly with Magnetic Field Bucking Coil Around Anode Channel.

Fig. 11 Mirror Field with Bucking Coil Energized.

Fig. 12 Variation of Electron Saturation Current, Operating Pressure, and Anode Magnetic Field with Midplane Magnetic Field.

Fig. 13 Midplane Density Profile for Two Arcs.

ORNL DWG. 66-6336

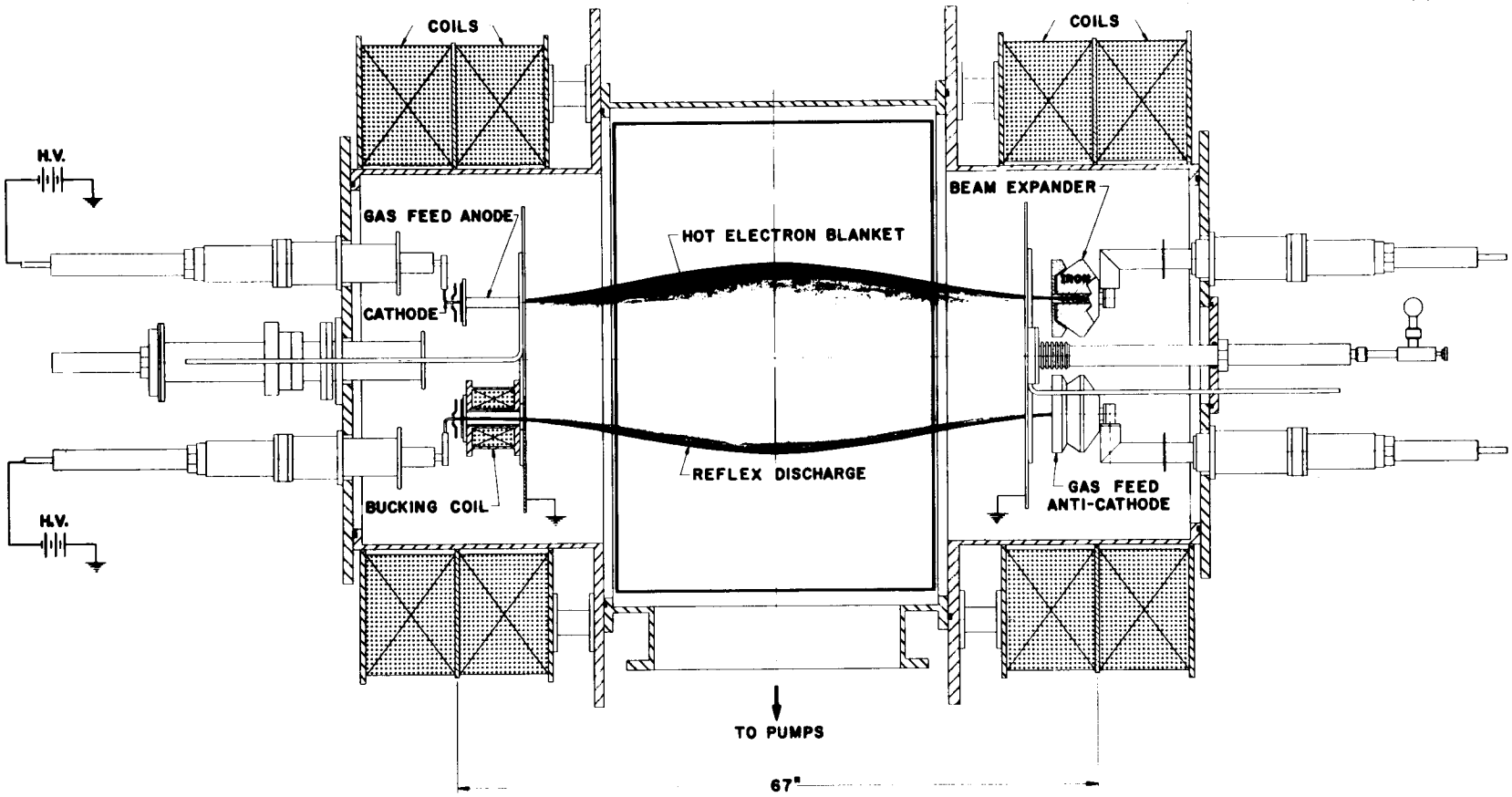

BEAM PLASMA FACILITY

Fig. 1

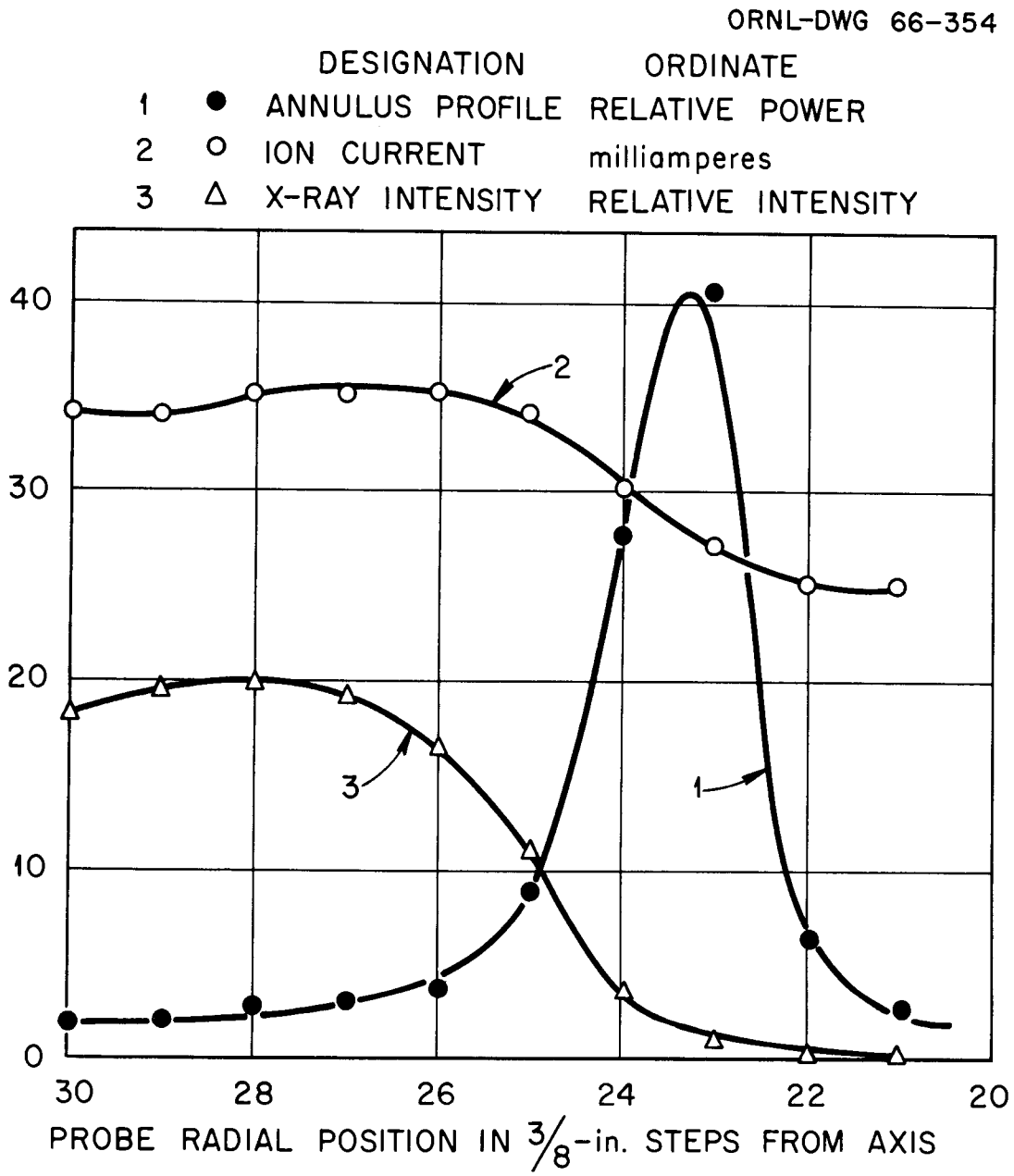
ORNL-DWG 66-354
DESIGNATION
ORDINATE
1 ANNULUS PROFILE RELATIVE POWER
2 ION CURRENT milliamperes
3 X-RAY INTENSITY RELATIVE INTENSITY
40
30
20
10
0
30
28
26
24
22
20
PROBE RADIAL POSITION IN 3/8-in. STEPS FROM AXIS
1
2
3

Fig. 2

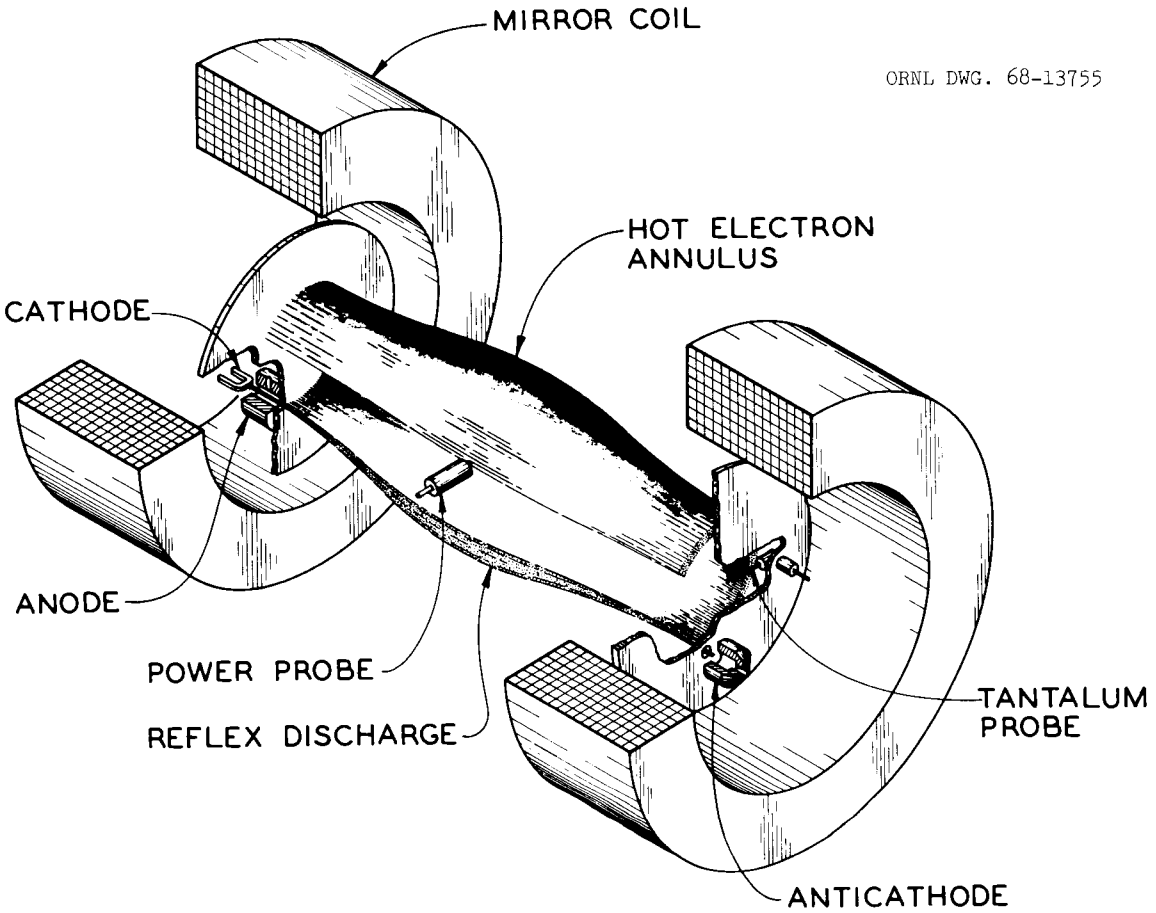

ISOMETRIC-SINGLE ARC OPERATION

Fig. 3

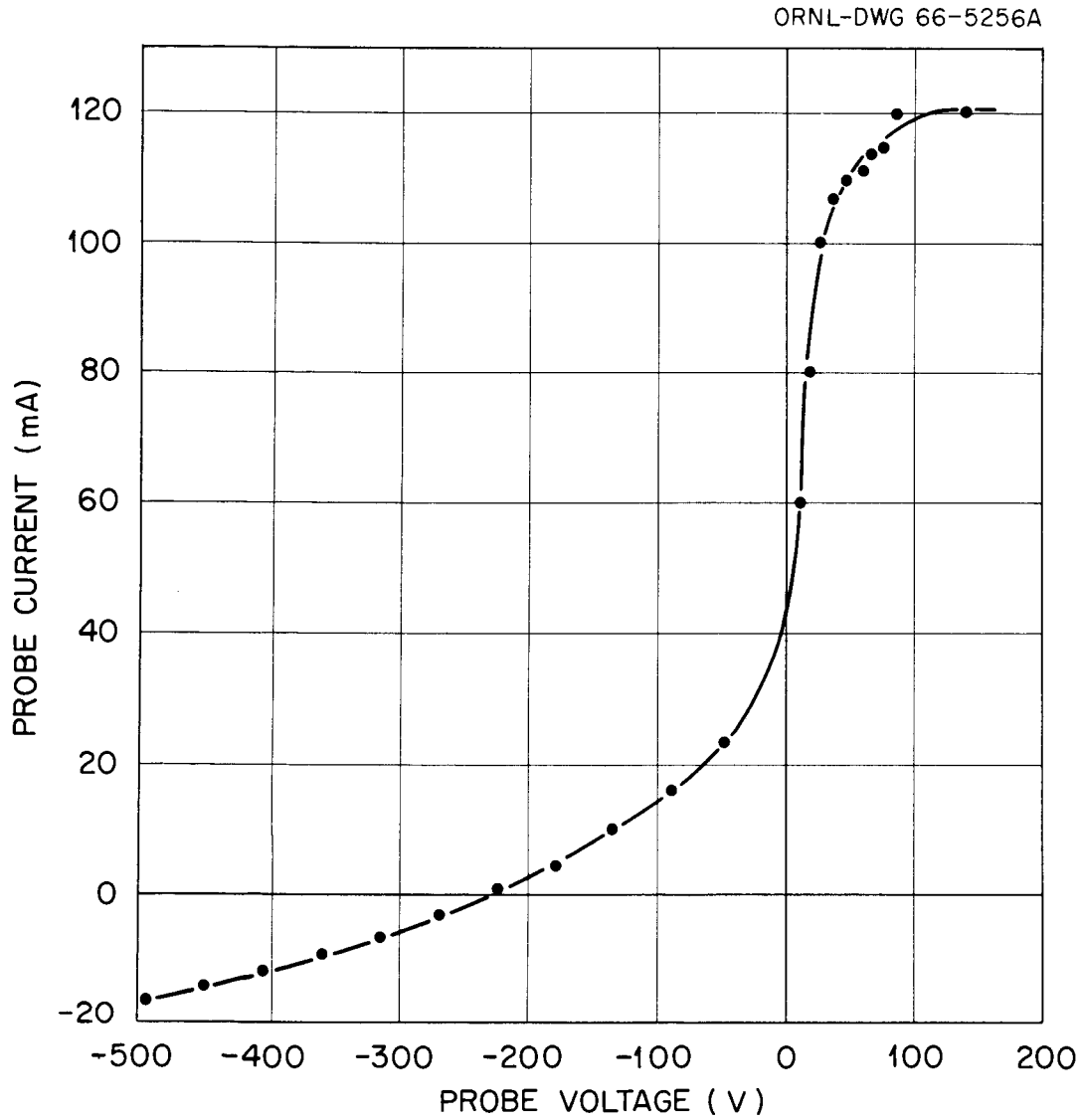
ORNL-DWG 66-5256A
PROBE CURRENT (mA)
120
100
80
60
40
20
0
-20
-500
-400
-300
-200
-100
0
100
200
PROBE VOLTAGE (V)

Fig. 4

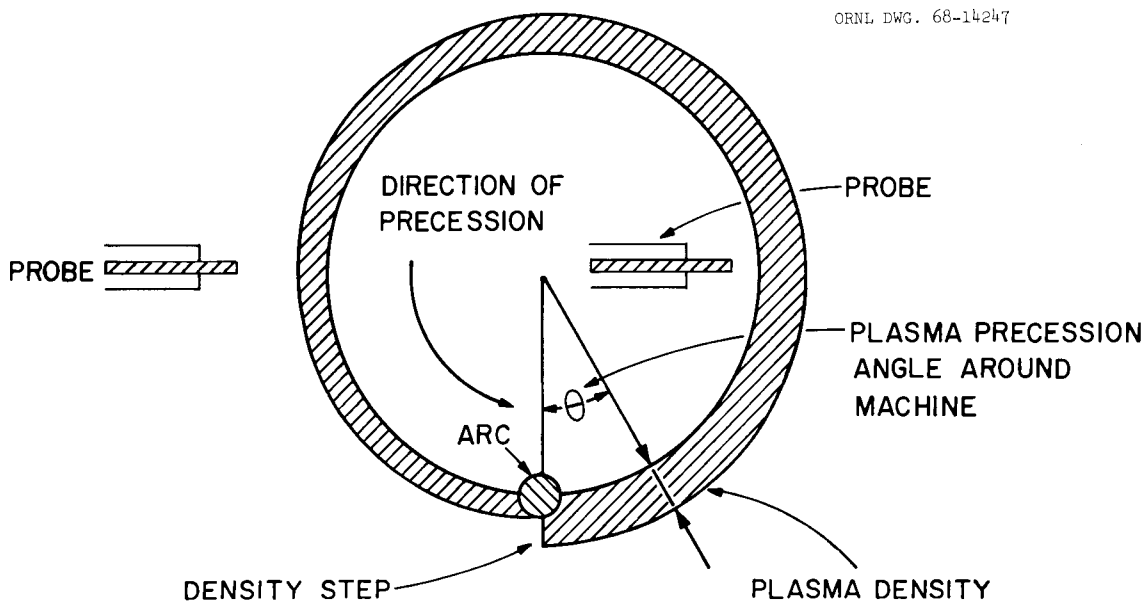
ORNL DWG. 68-14247
DIRECTION OF
PRECESSION
PROBE
PROBE
PLASMA PRECESSION
ANGLE AROUND
MACHINE
θ
ARC
DENSITY STEP
PLASMA DENSITY

Fig. 5

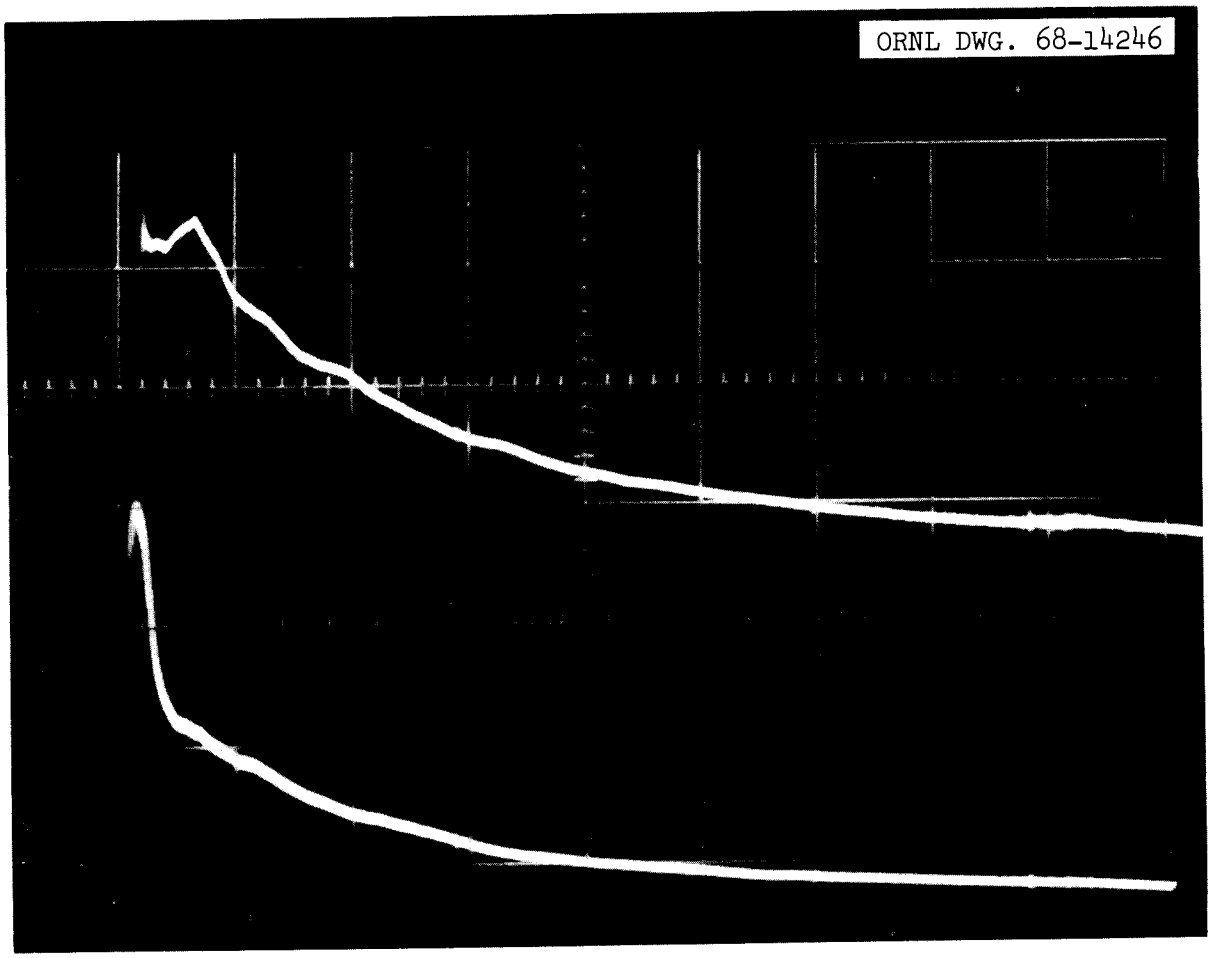

Time Scale, 100 μsec per Large Dimension

Fig. 6

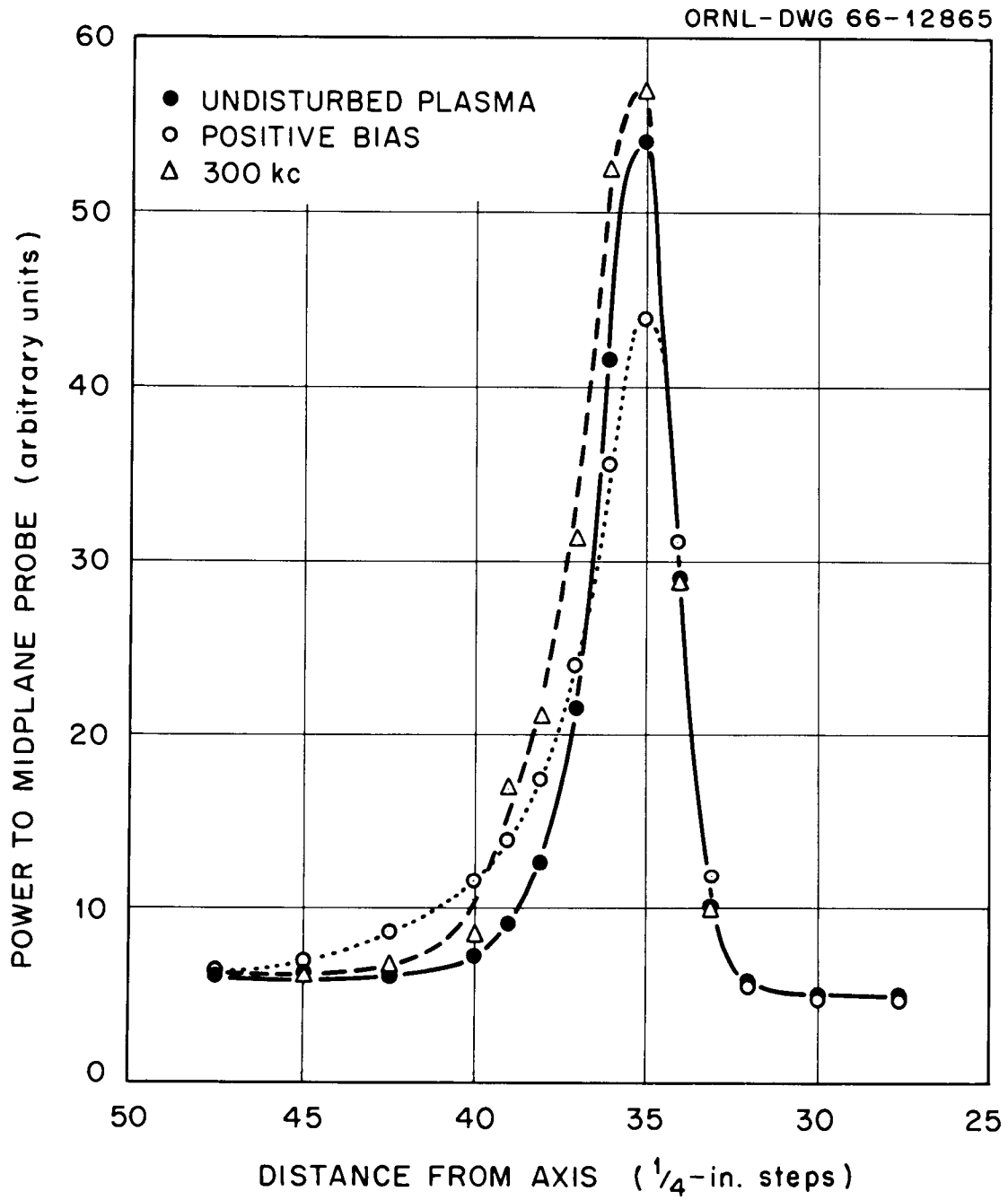
ORNL-DWG 66-12865
UNDISTURBED PLASMA
POSITIVE BIAS
300 kc
POWER TO MIDPLANE PROBE (arbitrary units)
DISTANCE FROM AXIS (1/4-in. steps)
0
10
20
30
40
50
60
50
45
40
35
30
25

Fig. 7

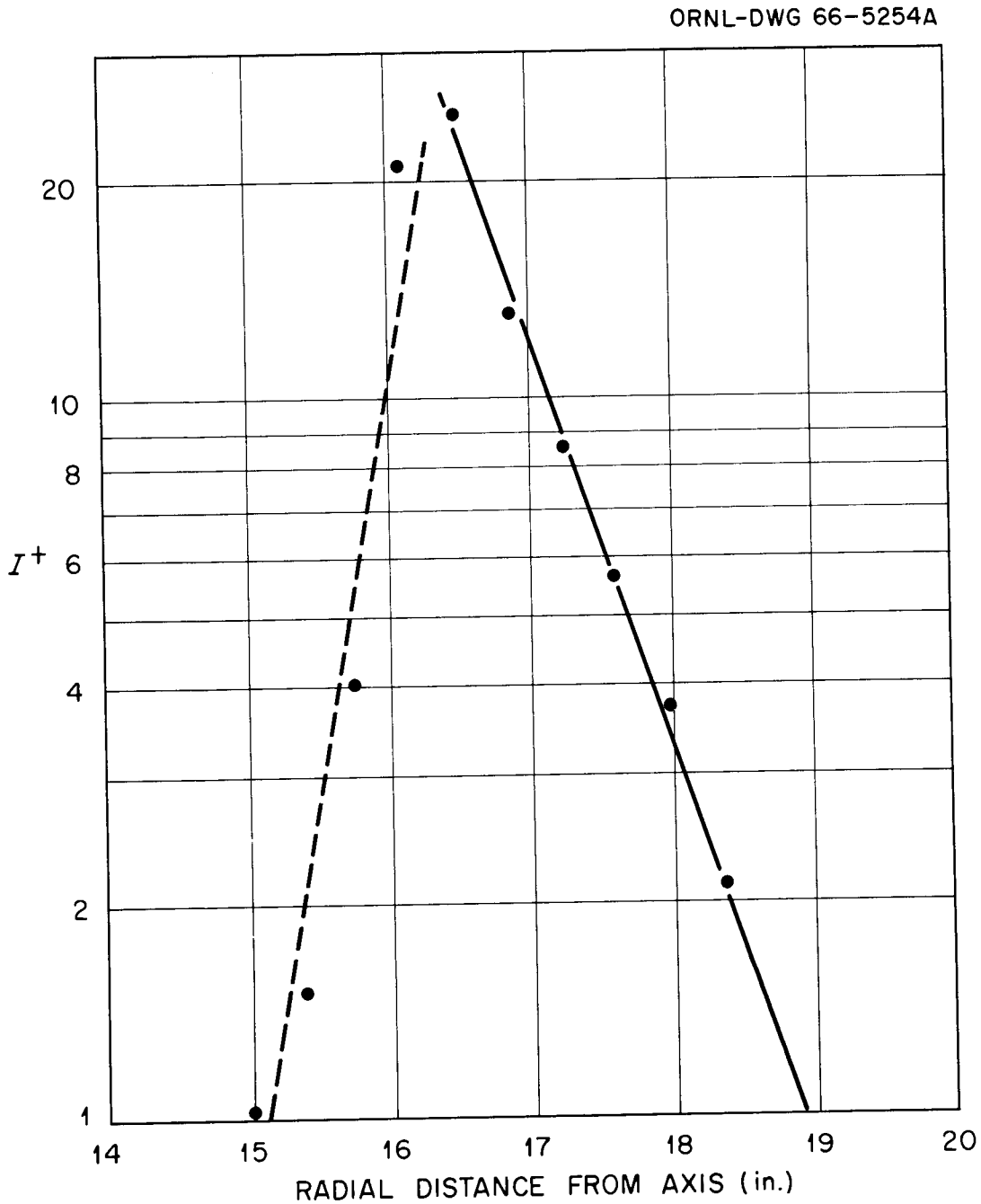
ORNL-DWG 66-5254A
20
10
8
I^+ 6
4
2
1
14
15
16
17
18
19
20
RADIAL DISTANCE FROM AXIS (in.)

Fig. 8

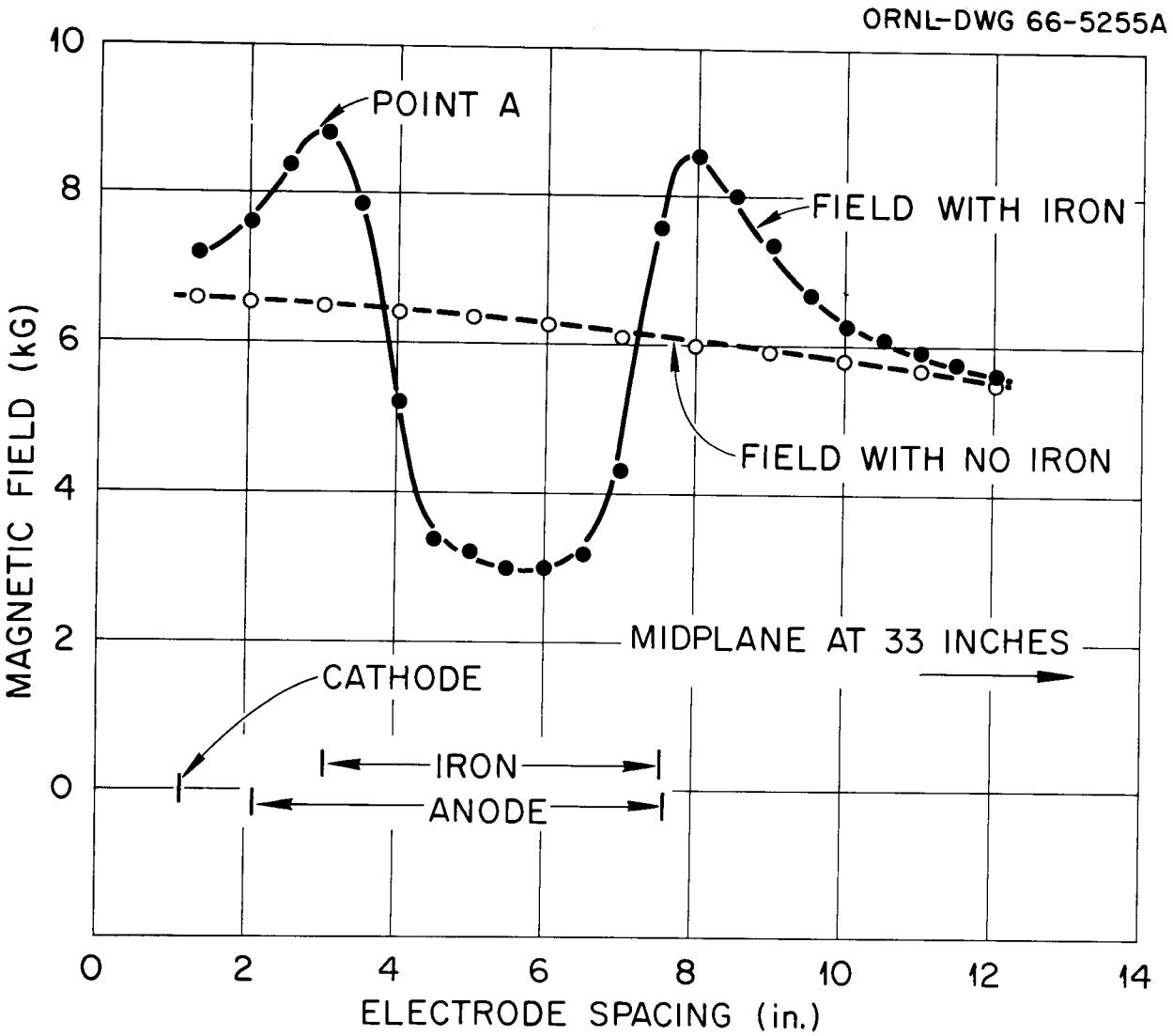
ORNL-DWG 66-5255A
POINT A
FIELD WITH IRON
FIELD WITH NO IRON
MIDPLANE AT 33 INCHES
CATHODE
IRON
ANODE
MAGNETIC FIELD (kG)
ELECTRODE SPACING (in.)
0
2
4
6
8
10
12
14

Fig. 9

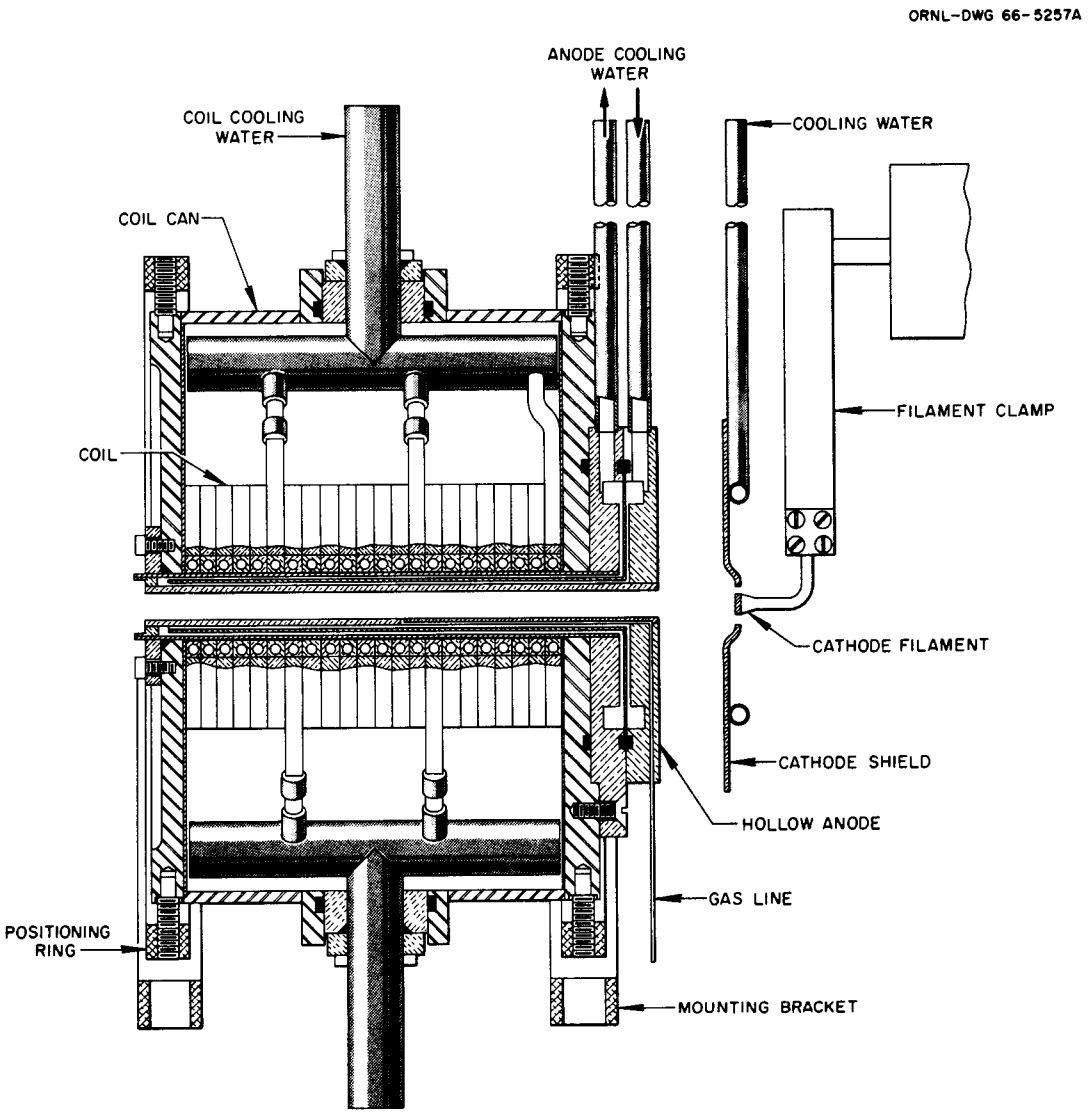
ORNL-DWG 66-5257A
ANODE COOLING WATER
COIL COOLING WATER
COOLING WATER
COIL CAN
FILAMENT CLAMP
COIL
CATHODE FILAMENT
CATHODE SHIELD
HOLLOW ANODE
GAS LINE
POSITIONING RING
MOUNTING BRACKET

Fig. 10

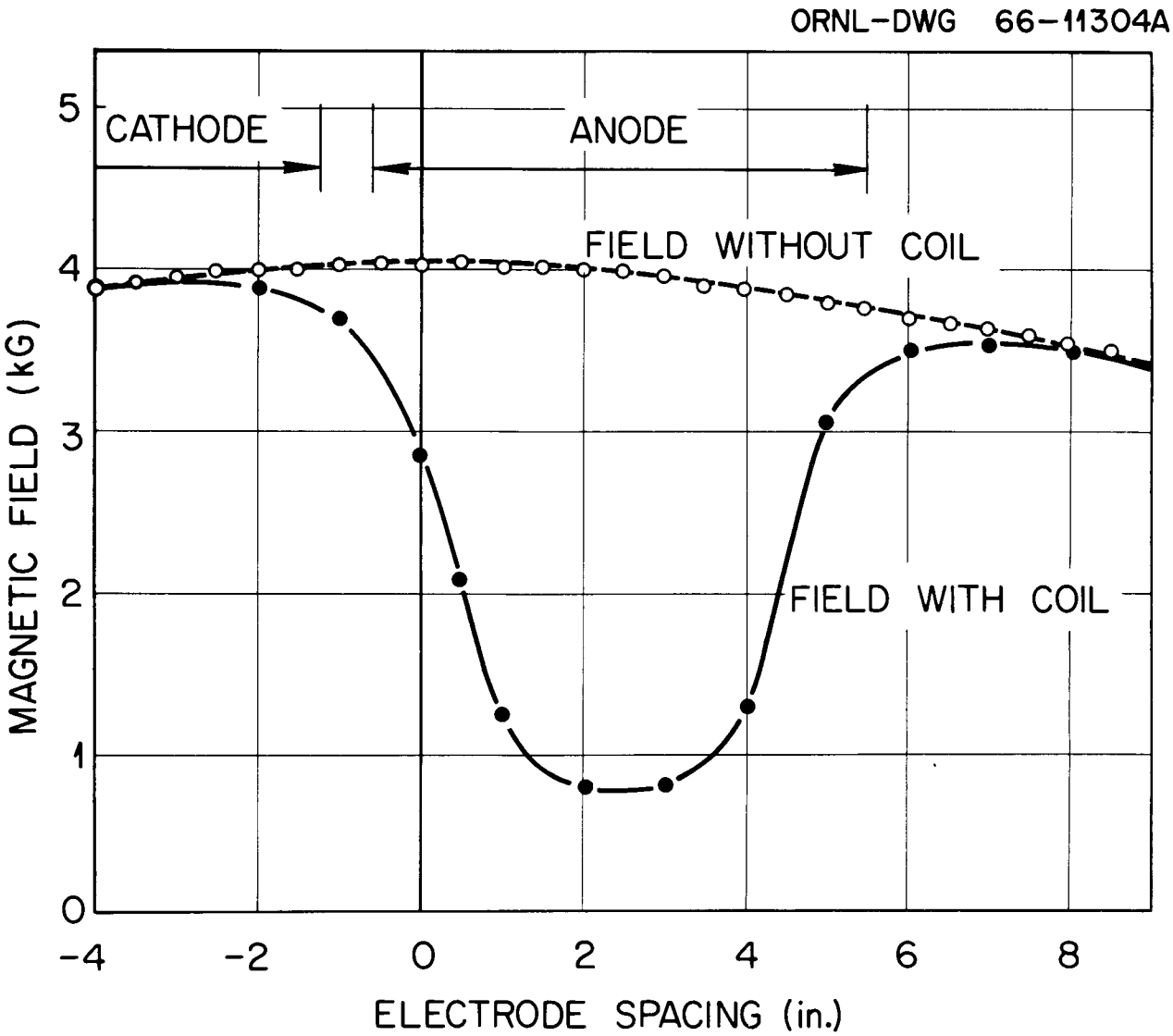
ORNL-DWG 66-11304A
CATHODE
ANODE
FIELD WITHOUT COIL
FIELD WITH COIL
MAGNETIC FIELD (kG)
ELECTRODE SPACING (in.)
0
1
2
3
4
5
-4
-2
0
2
4
6
8

Fig. 11

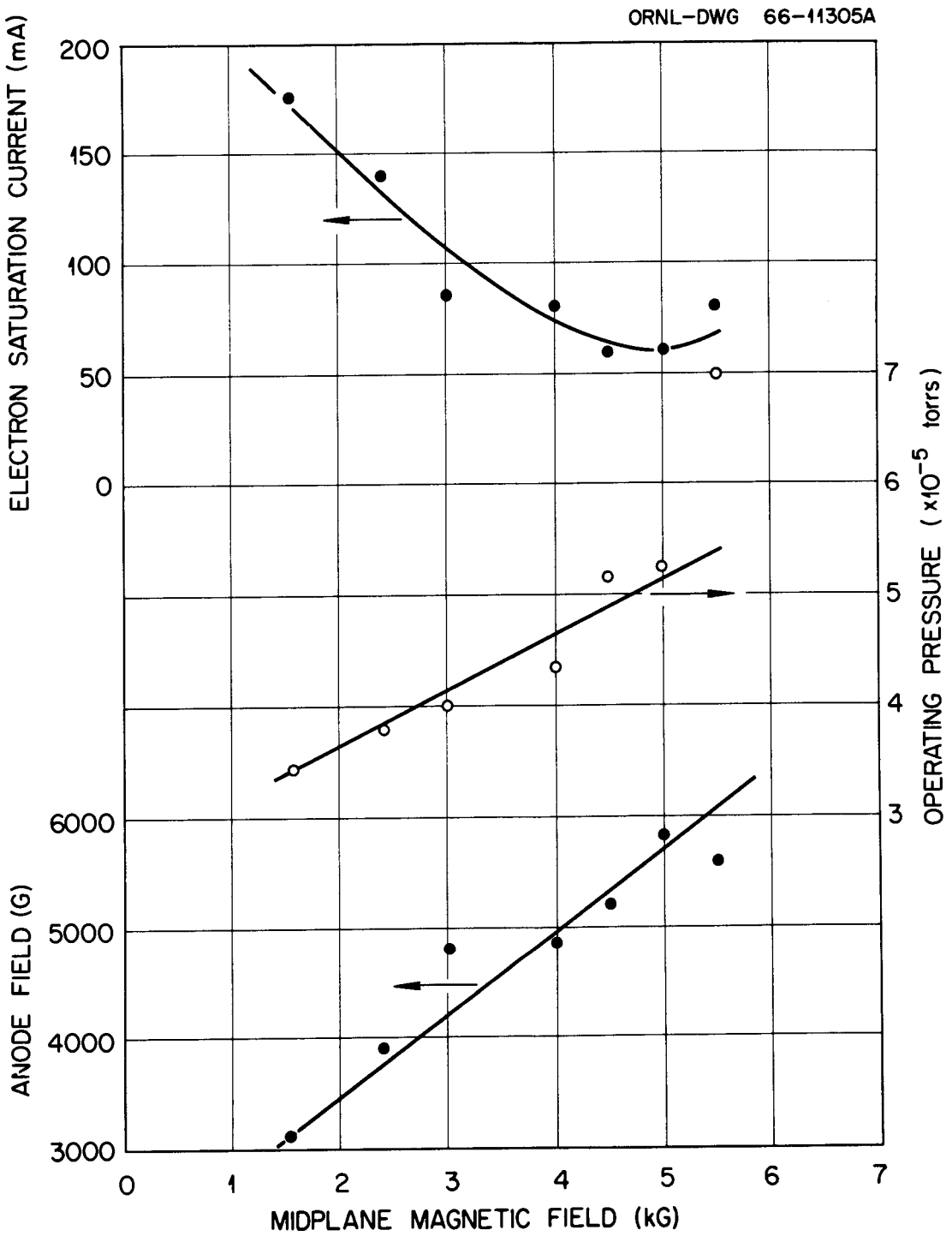
ORNL-DWG 66-11305A
ELECTRON SATURATION CURRENT (mA)
200
150
100
50
0
OPERATING PRESSURE (x10^{-5} torrs)
7
6
5
4
3
ANODE FIELD (G)
6000
5000
4000
3000
0
1
2
3
4
5
6
7
MIDPLANE MAGNETIC FIELD (kG)

Fig. 12

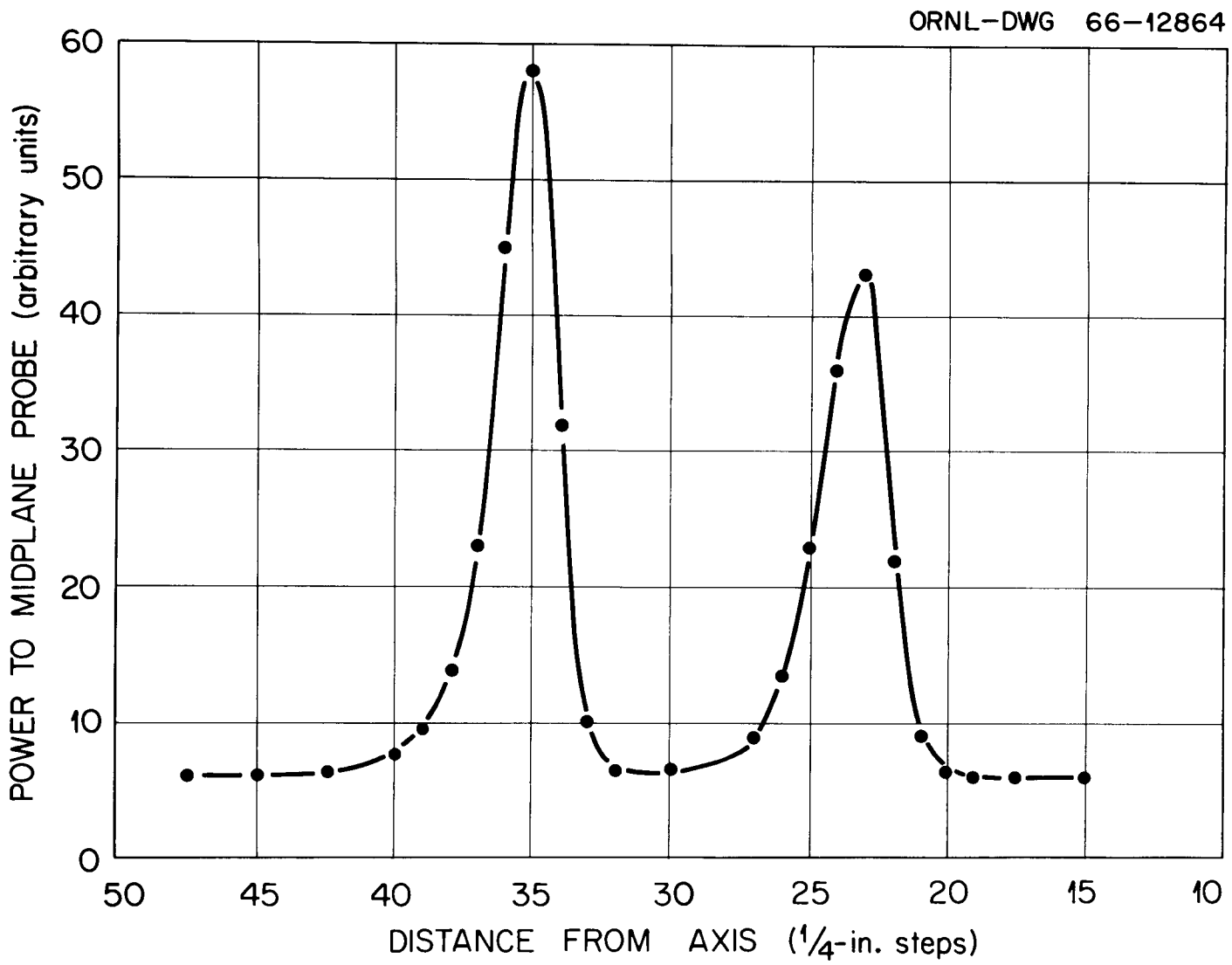
ORNL-DWG 66-12864
POWER TO MIDPLANE PROBE (arbitrary units)
60
50
40
30
20
10
0
50
45
40
35
30
25
20
15
10
DISTANCE FROM AXIS (1/4-in. steps)

Fig. 13